**ORIGINAL PAPER**

# Analysis of the spatial and temporal distribution of malaria in an area of Northern Guatemala with seasonal malaria transmission

Lucio Malvisi [1] · Catherine L. Troisi [1] · Beatrice J. Selwyn [1]

## Abstract

The risk of malaria infection displays spatial and temporal variability that is likely due to interaction between the physical environment and the human population. In this study, we performed a spatial analysis at three different time points, corresponding to three cross-sectional surveys conducted as part of an insecticide-treated bed nets efficacy study, to reveal patterns of malaria incidence distribution in an area of Northern Guatemala characterized by low malaria endemicity. A thorough understanding of the spatial and temporal patterns of malaria distribution is essential for targeted malaria control programs. Two methods, the local Moran's $I$ and the Getis-Ord $G^*(d)$, were used for the analysis, providing two different statistical approaches and allowing for a comparison of results. A distance band of 3.5 km was considered to be the most appropriate distance for the analysis of data based on epidemiological and entomological factors. Incidence rates were higher at the first cross-sectional survey conducted prior to the intervention compared to the following two surveys. Clusters or hot spots of malaria incidence exhibited high spatial and temporal variations. Findings from the two statistics were similar, though the $G^*(d)$ detected cold spots using a higher distance band (5.5 km). The high spatial and temporal variability in the distribution of clusters of high malaria incidence seems to be consistent with an area of unstable malaria transmission. In such a context, a strong surveillance system and the use of spatial analysis may be crucial for targeted malaria control activities.

**Keywords** Malaria · Spatial analysis · Clusters · Outliers · Moran's $I$ · Getis-Ord

## Introduction

The public health significance of malaria worldwide is substantial, with 216 million cases and 445,000 deaths in 2016 as reported by the World Health Organization (WHO 2017). Control measures to reduce malaria transmission, such as the use of long-lasting insecticide-treated bed nets, indoor residual spraying, vector management, and improved diagnostic tools and treatment have led to a considerable decline in the number of cases and deaths over the past decade (WHO 2017). However, in the dynamics of vector-borne disease transmission, the impact that the spatial and ecological characteristics of the physical environment have on malaria transmission is extensive, yet malaria control programs are often designed

and implemented giving these aspects little significance (Kitron 1998; Ostfeld et al. 2005). In malaria, the host (*Anopheles* mosquitos), the human, the agent (the *Plasmodium* parasite), and the physical environment are highly interdependent and different combinations of these elements affect transmission spatially and temporally (Grillet et al. 2010). As a result, a thorough knowledge and understanding of the spatial and temporal characteristics of malaria transmission dynamics are essential for developing suitable control programs at the local level and also for predicting future distribution patterns and outbreaks (Carter et al. 2000). To achieve this, it is critical to identify spatial patterns of distribution of malaria in the form of (1) clusters of high (hot spots) or low (cold spots) values (Jacquez 2008) and/or (2) outliers (Lu et al. 2003) and to reveal the underlying mechanisms responsible for such spatial phenomena.

While geographical information system (GIS) mapping tools help uncover such spatial phenomena visually, there are statistical techniques that can assess the statistical significance of these spatial patterns of aggregation of features. Two of the most common spatial analysis approaches that have

✉ Lucio Malvisi
luciomalvisi@hotmail.com

[1] Department of Epidemiology, Human Genetics & Environmental Sciences, School of Public Health, The University of Texas Health Science Center at Houston, Houston, TX, USA

been widely used to detect clusters and outliers in the field of malaria in areas of both stable and unstable transmission and for different purposes (Yeshiwondim et al. 2009; Bejon et al. 2010; Hui et al. 2009; Xia et al. 2015) are the local Moran's $I_i$ (Anselin 1995; Getis and Ord 1996) and the Getis-Ord $G_i^*(d)$ statistics (Getis and Ord 1992; Ord and Getis 1995). The combined use of both statistics is beneficial in that results can be compared, and more reliable and consistent conclusions can be drawn on the processes involved in spatial association (Getis and Ord 1992).

These two tests have been employed in this study to determine whether specific forms of spatial distribution of malaria incidence (i.e., as clusters or outliers) were present over an area of the Ixcán municipality in Northern Guatemala as opposed to a scenario of complete randomness in the spatial distribution of malaria incidence. The analysis involved three points in time corresponding to three cross sectional surveys (CTs) that were conducted in selected villages of this municipality between 2000 and 2001 as part of an insecticide-treated bed nets (ITNs) efficacy study (Malvisi 2015). Thus, besides an investigation of the spatial patterns of distribution of malaria incidence, a temporal evaluation that will span the three CTs (CT1, CT2, and CT3) has been presented. Of particular interest are the differences in terms of the spatial distribution of malaria incidence between the pre-intervention period during, which no villages had ITNs (CT1 and CT2), and the post-intervention period (CT3) when intervention villages had been using ITNs for the 9 months prior to CT3 while control villages had not. Implications for malaria control and considerations for future research are presented.

## Methods

### Study area

The spatial analysis covered villages of the Ixcán municipality (15° 59′ N, 90° 46′ W), which is part of the El Quiché Department in Northern Guatemala (Fig. 1). The Ixcán municipality has an extension of 1575 km$^2$ and the population was approximately 67,000 in 2000, comprising the municipal seat (Playa Grande) and 170 rural villages (Guatemala National Institute of Statistics, unpublished data). The area is characterized by lowlands with an average altitude of approximately 250 m above the sea level (Consejo Municipal de Desarrollo del Municipio de Ixcan, Quiche y Secretaria de Planificacion y Programacion de la Presidencia 2010), and the climate is hot and humid year-round with little temperature variations (mean temperature of 25.8 °C) (Instituto Nacional de Sismologia, Vulcanologia, Meteorologia e Hidrologia 2013; Narciso et al. 2013). Annual rainfall varies between 2000 and just over 3000 mm (Instituto Nacional de

Sismologia, Vulcanologia, Meteorologia e Hidrologia 2013). The area is bordered on the eastern and north-eastern side by the Chixoy River, the third longest river in the country and the site of the largest Guatemalan hydroelectric dam (Instituto Nacional de Electrificacion 2014).

Malaria transmission is unstable (entomological inoculation rate (EIR) < 1) and seasonal with higher intensity between May to October and a slight reduction between November and April (unpublished data, Guatemalan Institute of Seismology, Volcanology, Meteorology, and Hydrology). The majority of cases were caused by *P. vivax* (typically around 90%) with a small portion caused by *P. falciparum*. The primary malaria vectors according to an entomological survey carried out in the study villages between June 2000 and August 2001 were *An. vestitipennis* (41.2%), *An. darlingi* (37.5%), *An. Apicimacula* and *An. punctimacula* (13.4%), *An. albimanus* (7.1%), and *An. pseudopuncipennis* (0.4%).

### Epidemiologic and spatial data

All data used for the spatial analysis were collected during the ITN efficacy study conducted between 2000 and 2001. This study collected data on 9989 individuals from 26 villages over three cross-sectional surveys (approximately 1/3 of them were surveyed in each CT and individuals that participated in one CT could not be selected for the following ones). A detailed description of the experimental conditions of the efficacy study is found elsewhere (Malvisi 2015). Village-specific incidence rates of malaria (defined as the number of new cases divided by the population at risk and multiplied by 100) were obtained and used as the attribute value for each village for the spatial analysis and were obtained for all three cross-sectional surveys. In addition, the geographical coordinates for the midpoint of each village were obtained using ArcGIS® software and served as the "reference points" to determine the distances that defined a neighboring area for each village. These distance bands and their associated weights were then used in the calculation of the local Moran's $I_i$ and Getis-Ord $G_i^*(d)$ statistics.

Besides the two tests for the identification of clusters and outliers, we also assessed the global spatial autocorrelation which indicates whether malaria rates (each village has a rate associated with it) are randomly distributed or whether they are found in the form of clusters over the study area. The details are discussed in the next section.

### Analysis of global spatial and spatio-temporal associations

We assessed the presence of patterns of spatial association over the whole study area with the global spatial autocorrelation tool which calculates the global Moran's $I$ index. This tool uses the geographical position of villages, their associated

**Fig. 1** Location of Guatemala in Central America (upper map) and location of the Ixcán within Guatemala (lower map)



## Spatial cluster and outlier analysis

attributes (malaria incidence rates), and a selected distance band that defines a neighboring area for each location to determine whether these attribute values are randomly distributed (null hypothesis) over the whole study area or whether they aggregate in the form of clusters. We calculated the global Moran's index for several distance bands and evaluated the significance of the indices by calculating the $z$ score and the $p$ value. The higher the $z$ score (and the lower the $p$ value) at a specific distance band, the higher the probability that high or low incidence rates of malaria are spatially clustered in the study area being evaluated. A further useful element that provides valuable information is the assessment of the relationship between global Moran's $I$ and time. The temporal trend for the global spatial association of malaria rates was examined through a linear regression model containing the values of global Moran's $I$ at the 3.5-km distance band and the three points in time corresponding to CT1, CT2, and CT3.

The identification of spatial clusters over the village area was carried out using both the local Moran's $I_i$ (Anselin 1995) and Getis-Ord $G_i^*(d)$ statistics (Getis and Ord 1992), while the detection of outliers was achieved through the local Moran's $I_i$ only since the Getis-Ord $G_i^*(d)$ is not able to identify this type of spatial phenomenon. Of note, while statistical analysis packages that calculate the $G^*(d)$ statistic report clusters that are significant at the 90, 95, and 99% confidence intervals, in this study and for all the maps, we only included clusters of either high or low values that were significant at the 99 and the 95% confidence interval. In a context as that of this research where multiple comparisons need to be carried out due to the assessment of the relationship among features for each location in the data, the probability of rejecting one or more null hypotheses when they are, in fact, true (type I error rate) is typically

higher; therefore, the use of a 90% confidence interval may be inappropriate (Caldas de Castro and Singer 2006).

For both statistics, a key element is weight which is represented by a weight matrix whose values are determined by the type of spatial relationships chosen to represent the spatial features being analyzed. This, in practice, specifies how the distance between two locations should be defined (Caldas de Castro and Singer 2006; Esri 2012). In general, the higher the distance between two locations, the lower their weight and, consequently, their impact on the statistic.

In addition to the spatial analysis for the identification of clusters and outliers, we examined the space-time relationship of malaria incidence to account for the variation in the distribution of malaria incidence at different points in time (corresponding to the three CTs). For this evaluation, we created a single three-dimensional map in which the spatial phenomena can be observed over time, with time being the third dimension used to reproduce the temporal progression. In practice, the oldest results (CT1) are displayed closest to the ground, while more recent ones appear at higher levels and closer to one's view. The 3D representation of the results of the space-time analysis was created with ArcGlobe, a feature of ArcGIS®.

## Selection of distance defining a neighbor

A central aspect in cluster analysis is the definition of the spatial relationship among points (villages in this case) and the identification of the ideal distance that defines a neighbor for each location, keeping in mind that the selected distance should have the goal of maximizing the likelihood of detecting clusters or outliers (Esri 2012). The selection of what is considered a neighboring area for each location should reflect the dynamic interaction that exists between people, mosquitoes, and the physical environment since these elements can influence the risk of malaria spatially and temporally (Caldas de Castro et al. 2007). To achieve this, the first factor to consider is the geographical distribution of the villages, which helps in the selection of a sufficiently large distance to include an appropriate number of neighbors (at least one). Since villages are frequently located a few kilometers apart (Fig. 2) (average distance of 3.1 km), it would be appropriate to opt for a distance that is greater than 3.1 km. In addition, since having more than one neighbor is helpful in cluster analysis, by selecting a distance greater than 3.1 km leads to including more than one neighbor for each location. The second factor is the presence of control measures implemented in the villages which, in this case, is represented by the use of ITNs in the intervention villages in CT3 (through the ITN efficacy study).
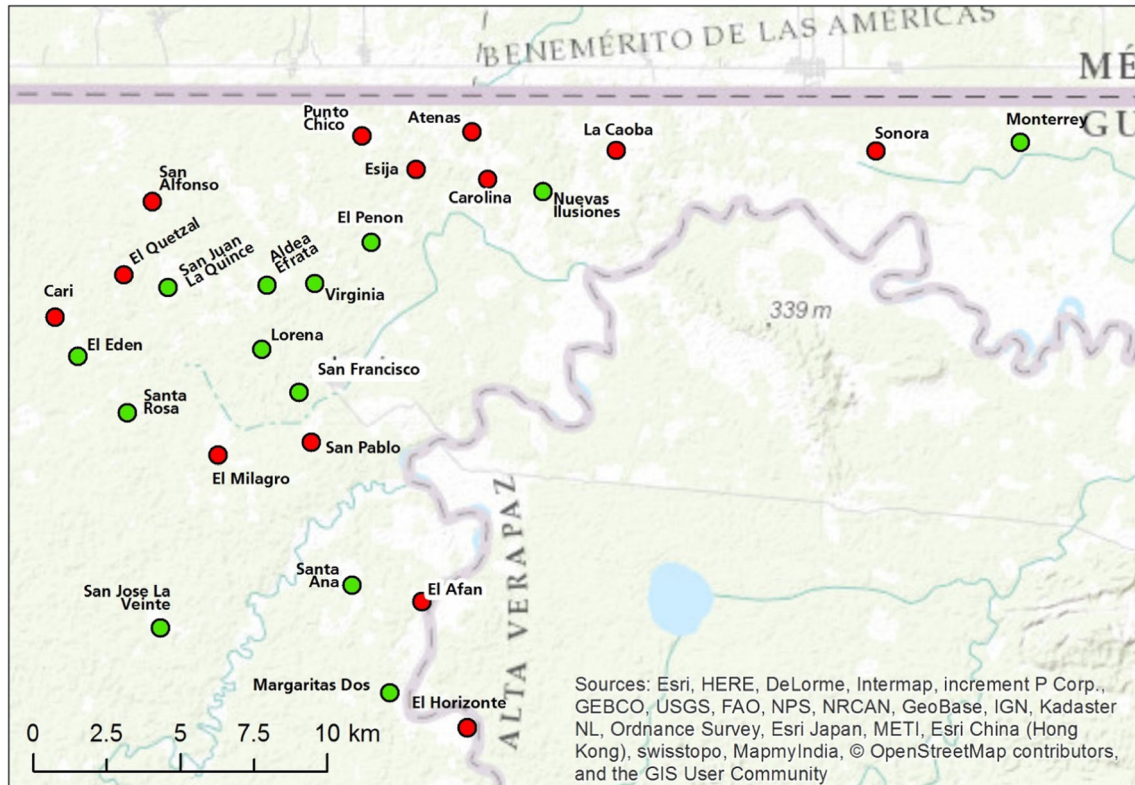


**Fig. 2** Villages included in the spatial analysis. Green dots symbolize intervention villages (those that received ITNs) and red dots represent control villages (no ITNs distributed)

As such, the presence of neighboring ITN and control villages as well as that of an area in which neighbors are ITN-ITN and control-control villages would be important to investigate spatial patterns of malaria in the presence of these combinations. The third element concerns the flying behavior of the mosquitoes: it was determined that *An. darlingi* can fly distances of up to 7 km, *An. albimanus* can reach 4.3 km, while *An. Vestitipennis* typically displays shorter ranges (< 1 km) (Fisher 1923; Verdonschot and Besse-Lototskaya 2014), although another study conducted in Belize concluded that there was a higher chance that *An. vestitipennis* traveled longer distance than to *An. albimanus* (Achee et al. 2007). Given this information and considering that data on distances traveled by these malaria vectors are limited and scattered, it is appropriate to select a distance slightly higher than 3 km but probably not too much higher. The forth factor is the result of the incremental spatial autocorrelation tool in ArcGIS® software. This procedure scans the area in which the spatial analysis is being performed and determines the distance at which the $z$ score for the global Moran's $I_i$ is maximized. According to this tool, this distance was 3.5 km. After a careful evaluation of all these factors, the most appropriate distance band defining a neighboring area was determined to be 3.5 km. This distance, in practice, defines a circular area with a diameter of 3.5 km around the geographical midpoint of each village. Therefore, this circular area represents the neighboring area for each reference village (we refer to a village that is the central point of this circular area as the reference village). Any village whose geographical midpoint falls within this circular area is a neighbor for the reference village. Besides the 3.5-km distance band, a few other distance bands consistent with the specific epidemiologic context of the different CTs were assessed and presented in the results section.

### Spatial weights

For the analysis, we used the fixed distance band approach so that locations that fall outside of the specified distance have weight of 0, i.e., they will not have an influence on the calculation of the statistic. In addition, since the number of neighbor villages for each village is different (some have only one

neighbor while others have up to fore), we used row standardized weights to create proportional weights for neighbors. In this way, a location that only has one neighbor will have a weight of 1 for its neighbor, while for a location that has more than one neighbor, the weights sum up to 1 for all neighbors.

### Split of isolated villages

As mentioned, the calculation of the local Moran's $I_i$ and Getis-Ord $G_i^*(d)$ statistics requires that each village has at least one neighbor and that a meaningful distance around each village is selected to define its neighboring area. The closest neighbor for some of the villages was located at distances greater than 5 km but selecting such high distances for a neighbor would have been inappropriate considering the entomological and geographical factors discussed above. To compensate for such a geographical context, we divided the six villages that had no neighbors within a 3.5-km distance into two sections so that each section had the other section of the village as its (only) neighbor. The split was applied near the geographical center of each of these six villages and following the most natural separation such as an area with no houses or a major road. The split villages were San Jose La Veinte, El Horizonte, Santa Ana, La Caoba, Sonora, and Monterrey. Following the split, the two sections in which each of these villages was split were named with the numbers 1 and 2 after the name of the village, e.g., Monterrey 1 for one section and Monterrey 2 for the other section (see Figs. 6, 7, 8, 9, 10, 11 for graphical example). The total number of locations after splitting these villages was 32.

## Results

### Characterization of malaria distribution in the three cross-sectional surveys

The local context of unstable and seasonal malaria transmission is reflected by the incidence rates that differ not only temporally (across CTs) (Table 1) but also spatially from one village to another one in close proximity, e.g., a few

Table 1 *P. vivax* cases, *P. falciparum* cases, total number of cases, and incidence rates of malaria in the three CTs

| Cross-sectional survey | PV[a] cases (%) | PF[b] cases (%) | Total cases | N[c] | IR[d] |
|---|---|---|---|---|---|
| CT1 | 220 (83.6) | 41 (15.6) | 263[e] | 3309 | 7.9 |
| CT2 | 54 (84.4) | 10 (15.6) | 64 | 3330 | 1.9 |
| CT3 | 68 (95.8) | 3 (4.2) | 71 | 3350 | 2.1 |

[a] *P. vivax* case % = number of cases of PV/total number of all cases

[b] *P. falciparum* case % = number of cases of PF/total number of all cases

[c] Population at risk

[d] Incidence rate calculated as: (total number of cases / total population) × 100

[e] Included in the 263 cases are also two mixed *P. falciparum/P. vivax* infections

kilometers away (Table 2 and Fig. 2). There were a total of 398 cases of malaria reported over the three CTs, with CT1 having the highest malaria rate (7.9 per 100 people) and the other two CTs having substantially lower rates, 1.9 and 2.1 per 100 people, respectively. Specifically for CT3 (conducted at the end of the intervention study period in which intervention villages had received ITNs, while control villages did not), the incidence rates of malaria for the ITN and control villages were 2.7 and 1.5 per 100 people, respectively (rate ratio = 1.81, 95% CI 1.11–1.92). The proportion of cases of *P. falciparum* malaria in both CT1 and CT2 was 15.6%, which was higher than that of CT3 (4.4%). The rest of the cases in all CTs were caused by *P. vivax*, except for two cases in CT1 which were diagnosed as mixed *P. falciparum/P. vivax* infections (Table 1). The distribution of malaria by age in CT1 shows no differences across age groups, while for CT2 and CT3, there was a significantly higher rate of malaria in

children aged 0 to 5 years than in those aged 6–15, 16–50, and more than 50 years ($p < 0.0001$) (Table 3). Finally, no statistically significant differences were observed in terms of malaria distribution by sex in any of the three cross-sectional surveys (data not shown).

## Spatial and temporal distribution of malaria

The spatial distribution of malaria incidence in the 32 locations over the three CTs is shown in Fig. 3. Here, we can confirm visually that the rates of malaria in CT1 appear higher than those in CT2 and CT3, while those of CT2 and CT3 appear similar. Spatially for CT1, the highest rates were observed in the northern and north-western parts of the study area, near the border with Mexico. For CT2, areas with higher rates of malaria are more evenly distributed over the study area with slightly higher concentrations in the central part as

**Table 2** Population, number of malaria cases, and incidence rates in all study villages

| Village name | CT1 (Sep/Oct 2000) | | | CT2 (Jan 2001) | | | CT3 (Oct/Nov 2001) | | |
|---|---|---|---|---|---|---|---|---|---|
| | N[a] | C[b] | IR[c] | N[a] | C[b] | IR[c] | N[a] | C[b] | IR[c] |
| Aldea Efrata | 120 | 1 | 0.8 | 130 | 6 | 4.6 | 131 | 2 | 1.5 |
| Atenas | 188 | 55 | 29.3 | 156 | 3 | 1.9 | 195 | 1 | 0.5 |
| Cari | 70 | 1 | 1.4 | 54 | 2 | 3.7 | 7 | 0 | 0 |
| Carolina | 110 | 13 | 11.8 | 94 | 2 | 2.1 | 114 | 0 | 0 |
| El Afan | 156 | 1 | 0.6 | 218 | 8 | 3.7 | 175 | 3 | 1.7 |
| El Eden | 97 | 4 | 4.1 | 113 | 1 | 0.9 | 105 | 0 | 0 |
| El Horizonte | 105 | 3 | 2.9 | 95 | 2 | 2.1 | 83 | 1 | 1.2 |
| El Milagro | 69 | 5 | 7.2 | 88 | 3 | 3.4 | 69 | 7 | 10.1 |
| El Peñon | 58 | 13 | 22.4 | 81 | 6 | 7.4 | 60 | 0 | 0 |
| El Quetzal | 60 | 0 | 0 | 70 | 2 | 2.9 | 101 | 5 | 5 |
| Esija | 79 | 22 | 27.8 | 100 | 4 | 4 | 80 | 2 | 2.5 |
| La Caoba | 153 | 15 | 9.8 | 169 | 0 | 0 | 189 | 1 | 0.5 |
| Lorena | 148 | 11 | 7.4 | 104 | 1 | 1 | 148 | 0 | 0 |
| Margaritas Dos | 151 | 4 | 2.7 | 124 | 1 | 0.8 | 103 | 1 | 1 |
| Monterrey | 101 | 28 | 27.7 | 82 | 0 | 0 | 63 | 2 | 3.2 |
| Nuevas Ilusiones | 114 | 5 | 4.4 | 131 | 1 | 0.8 | 134 | 3 | 2.2 |
| Punto Chico | 183 | 12 | 6.6 | 202 | 3 | 1.5 | 195 | 1 | 0.5 |
| San Alfonso | 81 | 10 | 12.3 | 53 | 0 | 0 | 67 | 1 | 1.5 |
| San Francisco | 77 | 14 | 18.2 | 110 | 2 | 1.8 | 92 | 1 | 1.1 |
| San Jose La Veinte | 348 | 1 | 0.3 | 297 | 2 | 0.7 | 339 | 4 | 1.2 |
| San Juan La Quince | 108 | 5 | 4.6 | 162 | 3 | 1.9 | 154 | 14 | 9.1 |
| San Pablo | 271 | 5 | 1.8 | 269 | 1 | 0.4 | 268 | 1 | 0.4 |
| Santa Ana | 135 | 3 | 2.2 | 145 | 5 | 3.5 | 173 | 16 | 9.3 |
| Santa Rosa | 97 | 9 | 9.3 | 70 | 5 | 7.1 | 80 | 1 | 1.3 |
| Sonora | 151 | 21 | 13.9 | 110 | 0 | 0 | 116 | 2 | 1.7 |
| Virginia | 84 | 2 | 2.4 | 104 | 1 | 1 | 109 | 2 | 1.8 |
| Total | 3309 | 263 | 7.9 | 3330 | 64 | 1.9 | 3350 | 71 | 2.1 |

[a] Population at risk

[b] Number of malaria cases

[c] Incidence rate per 100 people

**Table 3** Incidence rate of malaria by age group in the three CTs

| Age group (years) | CT1 incidence rate | CT2 incidence rate[a] | CT3 incidence rate[a] |
|---|---|---|---|
| 0–5 | 7.8 | 3.9 | 3.3 |
| 6–15 | 8.3 | 1.7 | 1.9 |
| 16–50 | 7.6 | 0.7 | 1.4 |
| >50 | 8.3 | 1.0 | 1.5 |

[a] In CT2 and CT3, the rates of malaria in children aged 0 to 5 years were significantly higher than those in participants aged 6–15, 16–50, and more than 50 years ($p < 0.0001$)

compared with CT1. Similar to CT2, the highest rates in CT3 are dispersed over the study area even though we observe a reappearance of pockets of malaria in the central and southern part. Overall, there was a progressive reduction in incidence over the CTs in most villages (as illustrated by the 3D view of the study area in Fig. 4), and there are no consistent trends of malaria distribution over space and time.

## Global spatial autocorrelation

Table 4 and Fig. 5 illustrate the results of the global spatial autocorrelation in which the Moran's $I$ index and its associated $z$ score and $p$ value were calculated for each selected distance

(in km) and for each of the three CTs. For CT1, the spatial autocorrelation was highest at the 3.5-km distance lag as indicated by the $z$ score, although all distances examined were significant as per the $p$ value. The 3.5-km distance lag was also the distance at which the spatial autocorrelation was maximized for CT2 as indicated by the $z$ score and $p$ value; the 3.2-km distance lag was also significant ($p < 0.05$), while the other distances had lower $z$ score and were not significant according to the $p$ value. All Moran's $I$ values and $z$ scores for CT1 and CT2 were positive, indicating a type of distribution of values that tends toward a clustering of high values, although Moran's index values should not be interpreted according to their high or low value, instead they should be evaluated in the context of the null hypothesis (i.e., the $p$ value). The spatial autocorrelation scenario shown in CT3 was different from that of the first two CTs in that no distance lags produced significant results. In addition, the Moran's $I$ and $z$ score values for the 4.0, 4.5, and 5-km distance lags were negative, denoting possible aggregation of values in the form of spatial outliers. Since in the Getis-Ord $G_i^*(d)$ statistic the individual test results are not related to a global statistic of spatial association as for the Moran's $I$ statistic, no tests of the global spatial autocorrelation associated with the Getis-Ord $G_i^*(d)$ statistic can be calculated.

In terms of the temporal trend for the global spatial association of malaria rates (assessed using the global Moran's $I$
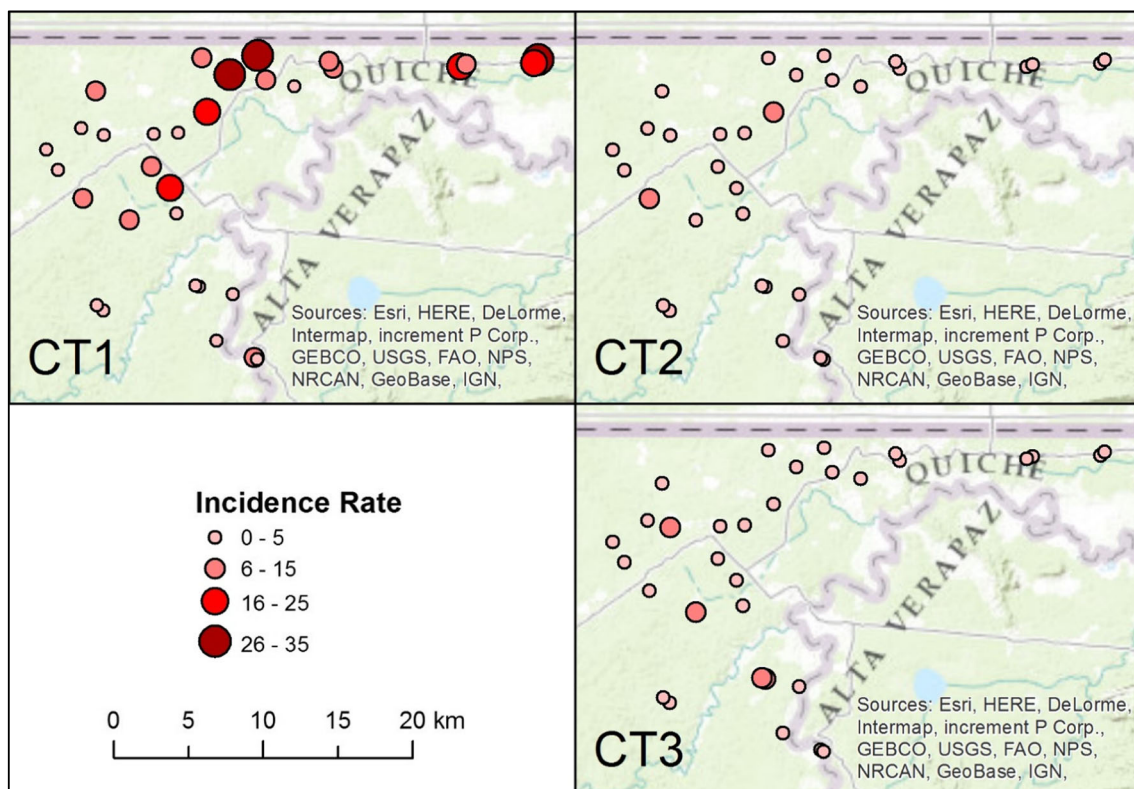
**Fig. 3** Incidence rates (per 100 population) of malaria for all villages in the three cross-sectional surveys (CT1, CT2, and CT3)

Fig. 4 Three-dimensional representation of malaria incidence rates (reported as the number of cases per 100 people) in villages over the three CTs. Each stick represents a villages and each CT is represented by one third of the length of the stick, with the lowest third corresponding to the incidence of the least recent CT and the highest third corresponding to the incidence of the most recent CT
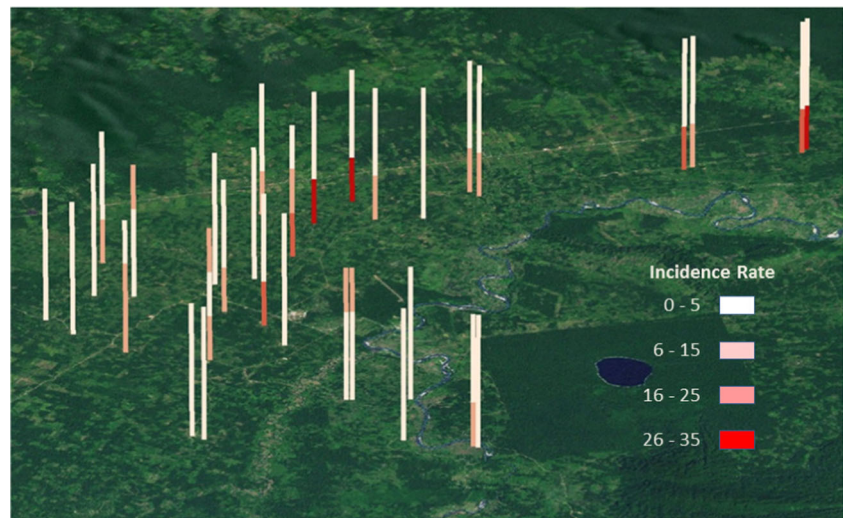


values at the 3.5-km distance band at the three points in time corresponding to CT1, CT2, and CT3), there was a significant decrease in the global Moran's $I$ values for the rates of malaria from CT1 to CT3 ($t = 5.85$, $p < 0.05$).

## Assessment of local spatial distribution of malaria incidence rates by the Moran's $I$ and Getis-Ord $G_i^*(d)$ statistics

### Cross-sectional survey I

Results from both the local Moran's $I$ (Fig. 6) and Getis-Ord $G_i^*(d)$ (Fig. 7) statistics at the 3.5-km distance lag show areas of significant clustering of high values of malaria incidence in the northern part of the study area with a highly significant cluster (99% CI) according to the Getis-Ord $G^*(d)$ statistic in the villages of Esija, as well as a cluster of high values in the village of Monterrey (north-west). However, Monterrey was one of the villages that was split and, thus, each section of Monterrey has as its only neighbor the other section of Monterrey (at the 3.5-km distance band), e.g., Monterrey 1 is the only neighbor for Monterrey 2 and vice versa. Thus, the interpretation of this particular cluster needs to take this

context into consideration. Notably, when we assessed the spatial distribution of malaria incidence using the $G^*(d)$ test with a 5.5-km distance lag, we observed an area of clusters of low values (cold spot) in the southern part of the study area.

### Cross-sectional survey II

Figures 8 and 9 display the results of the local Moran's $I$ and the Getis-Ord $G^*(d)$ statistics, respectively, using a 3.5-km distance lag. The former shows one significant cluster of high values of malaria incidence in the western area (Santa Rosa), while the latter indicates no significant clusters of either high or low values. Interestingly, according to the $G^*(d)$ statistic and using a distance band of 5.5 km, there was an area of significant low values of malaria incidence (cold spot) in the north-eastern part of the study area corresponding to the villages of Monterrey and Sonora. The former was a cluster of high values during CT1.

### Cross-sectional survey III

Spatial phenomena detected in CT3 are shown in Fig. 10 for the local Moran's $I$ and in Fig. 11 for the Getis-Ord $G^*(d)$

Table 4 Moran's $I$ index, $z$ score, and $p$ value for malaria incidence at different distance lags according to the spatial autocorrelation (global Moran's $I$). Results are presented for all CTs

| Distance | CT1 | | | CT2 | | | CT3 | | |
|---|---|---|---|---|---|---|---|---|---|
| | Moran's $I$ | $z$ score | $p$ value | Moran's $I$ | $z$ score | $p$ value | Moran's $I$ | $z$ score | $p$ value |
| 3.2 km | 0.48 | 2.82 | < 0.01 | 0.29 | 2.08 | < 0.05 | 0.07 | 0.61 | NS[a] |
| 3.5 km | 0.47 | 3.04 | < 0.01 | 0.26 | 2.15 | < 0.05 | 0.07 | 0.62 | NS[a] |
| 4.0 km | 0.41 | 2.88 | < 0.01 | 0.18 | 1.76 | NS[a] | −0.06 | −0.22 | NS[a] |
| 4.5 km | 0.35 | 2.76 | < 0.01 | 0.16 | 1.69 | NS[a] | −0.04 | −0.09 | NS[a] |
| 5.0 km | 0.42 | 2.89 | < 0.01 | 0.15 | 1.71 | NS[a] | −0.08 | −0.38 | NS[a] |

[a] Not significant

**Fig. 5** Z-score values for malaria incidence at different distance lags (in km) according to the spatial autocorrelation (global Moran's I). Results are presented for all CTs
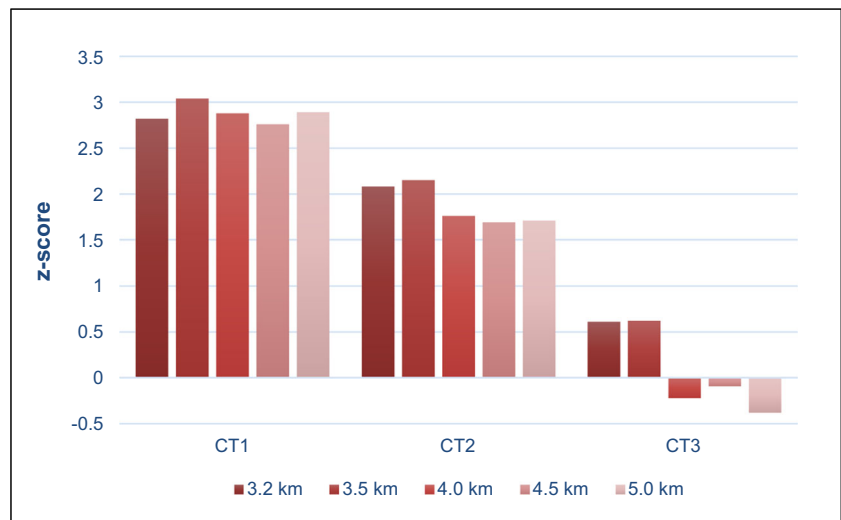


statistics. Both maps indicate a cluster of high values in the southern area, although a location identified as a cluster of high values of malaria incidence by both the local Moran's $I$ and the $G^{*}(d)$ corresponds to the two sides of one of the villages that was split (Santa Ana); therefore, the interpretation provided for the cluster of high values around Monterrey in CT1 can also be applied here. The local Moran's $I$ statistic also identified a spatial outlier, in this case an area with high incidence of malaria surrounded by an area of low incidence, in

the village of El Milagro which is located in the central part of the study area. Since this CT was conducted after the end of the intervention study period and due to the high presence of ITN villages in the central section of the study area, we also conducted a spatial analysis using both the local Moran's $I$ and the Getis-Ord $G^{*}(d)$ statistics with a distance band of 5.5 km to include control villages within the neighboring area of ITN villages and to determine whether different spatial phenomena would be observed. The local Moran's $I$ test identified the
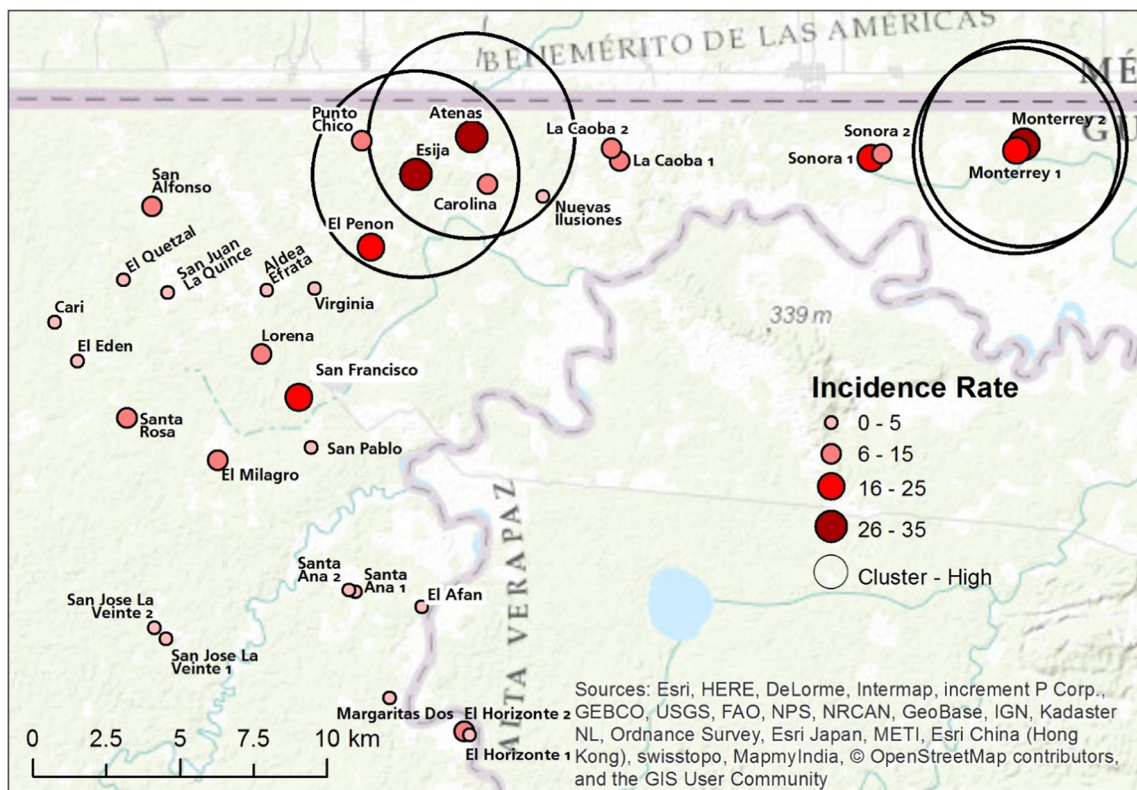


**Fig. 6** Map of villages showing results of the local Moran's $I$ statistic for CT1 (conducted between September and October, thus falling within the rainy season when more cases of malaria are expected to occur) using a 3.5-km distance band. Incidence rate = number of cases per 100 people
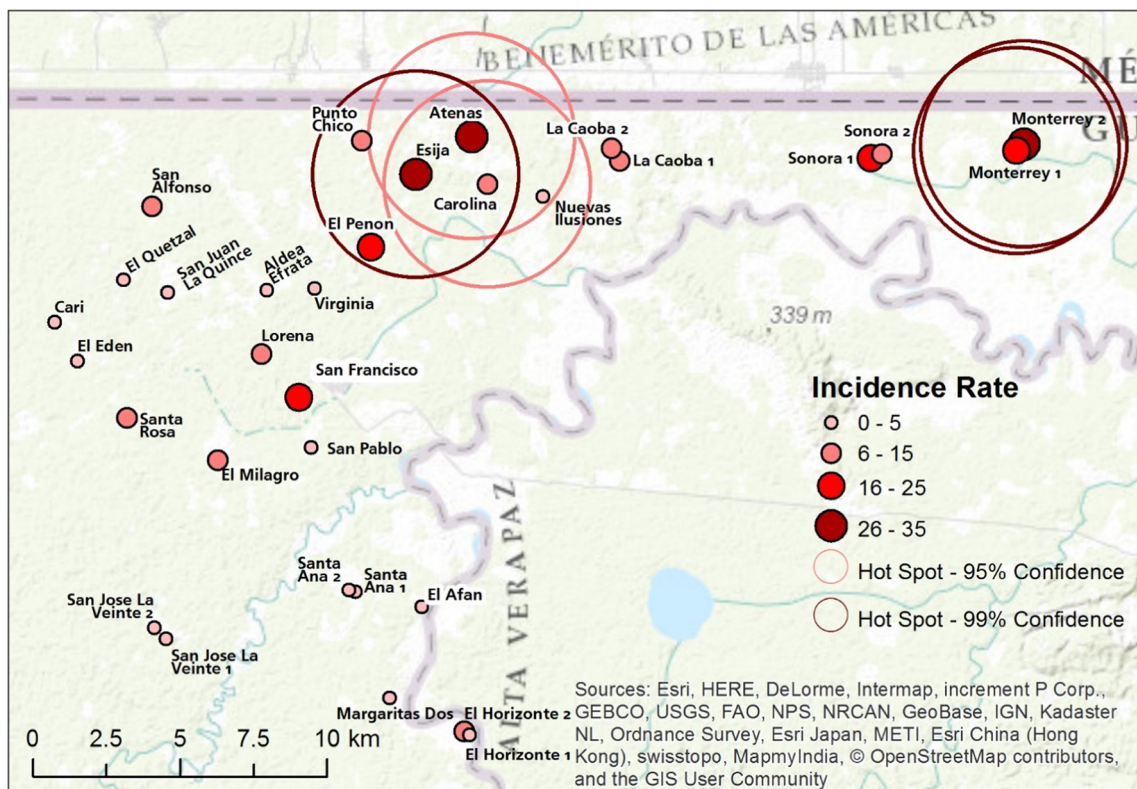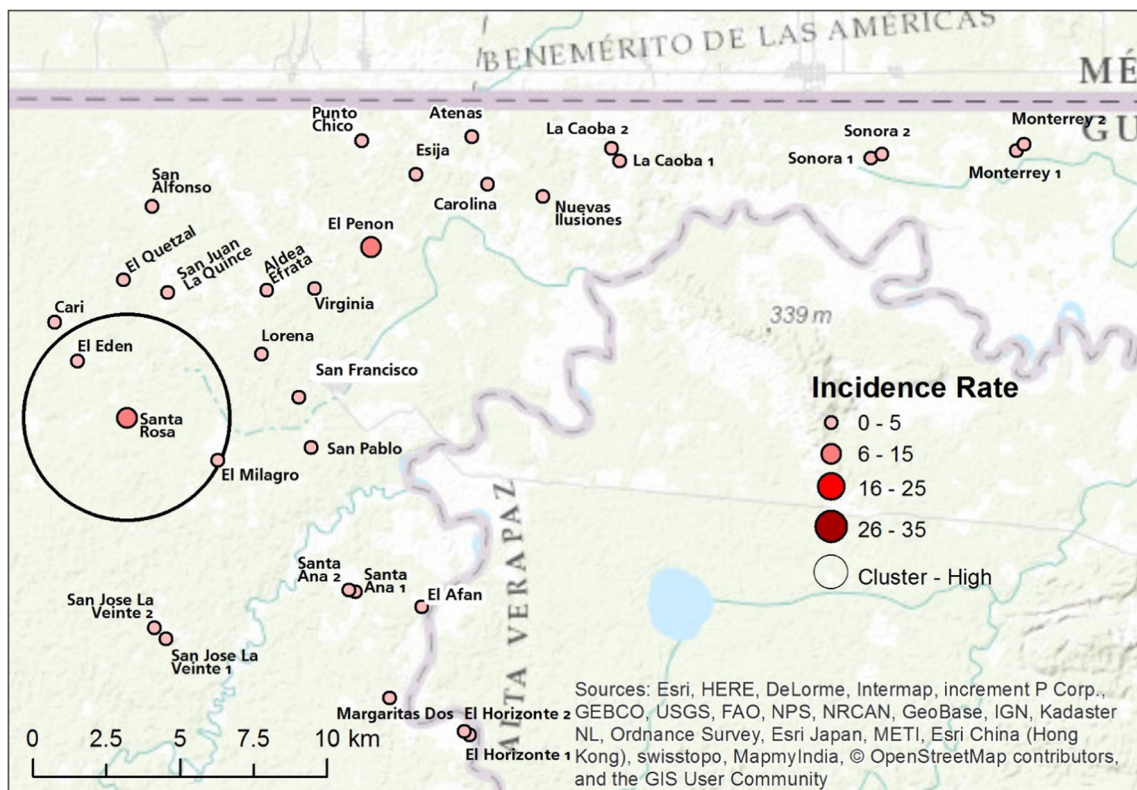
**Fig. 7** Map of villages showing results of the Getis-Ord $G^*(d)$ statistic for CT1 (conducted between September and October, thus falling within the rainy season when more cases of malaria are expected to occur) using a 3.5-km distance band. Incidence rate = number of cases per 100 people



**Fig. 8** Map of villages showing results of the local Moran's $I$ statistic for CT2 (conducted in January which falls during the dry season and a low number of cases of malaria are expected to occur) using a 3.5-km distance band. *Incidence rate = number of cases per 100 people
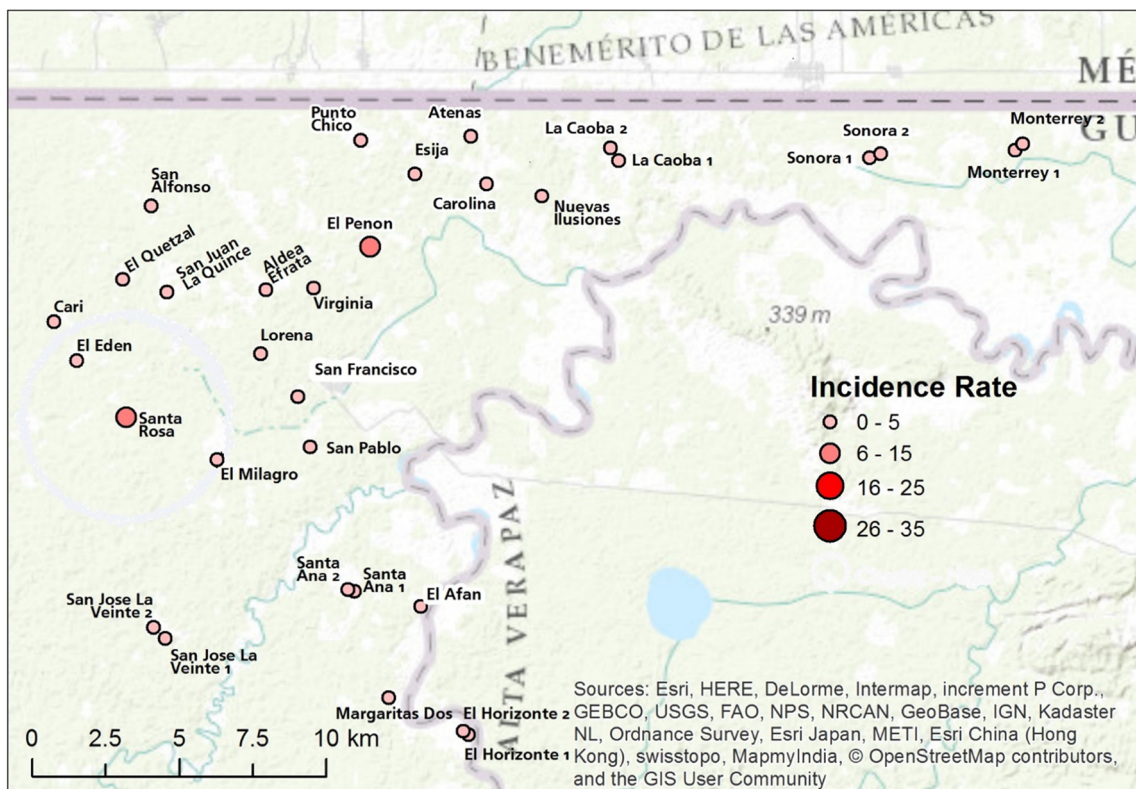
**Fig. 9** Map of villages showing results of the Getis-Ord $G^*(d)$ statistic for CT2 (conducted in January which falls during the dry season and a low number of cases of malaria are expected to occur) using a 3.5-km distance band. No clusters were detected. *Incidence rate = number of cases per 100 people
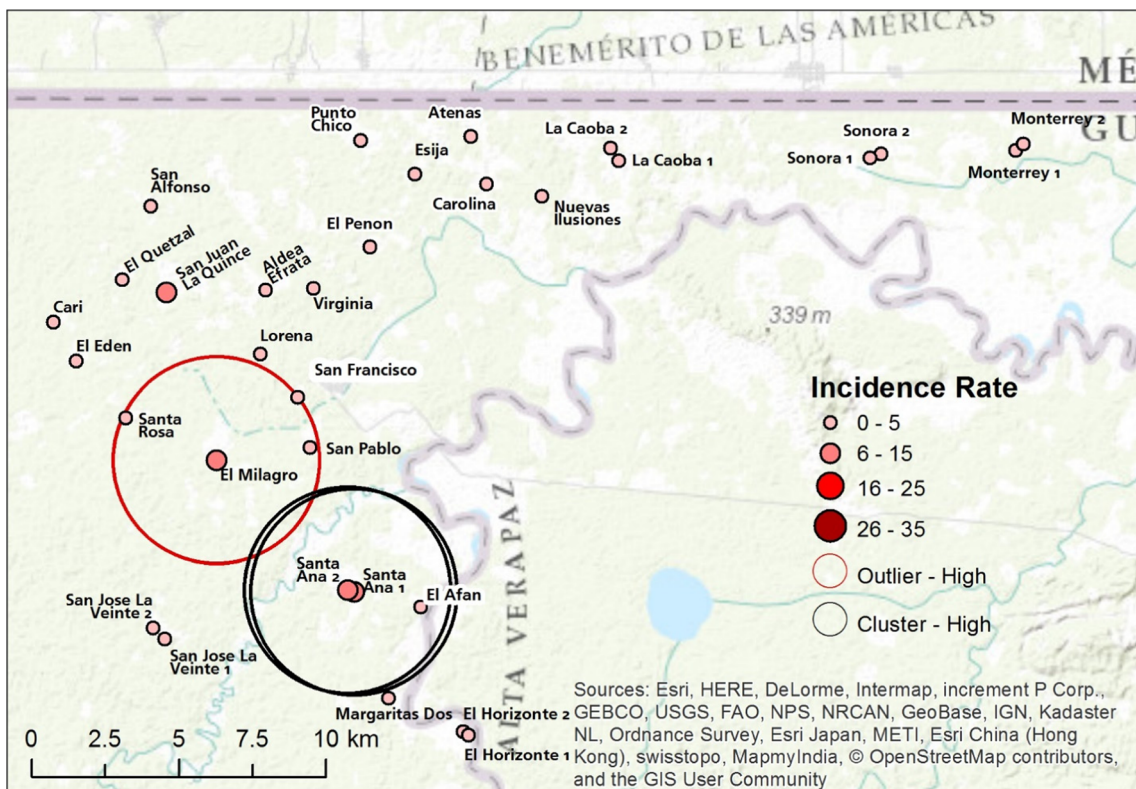


**Fig. 10** Map of villages showing results of the local Moran's $I$ statistic for post-intervention CT3 (conducted between October and November which correspond to the end of the rainy season and less cases of malaria may occur compared to the middle part of the rainy season) using a 3.5-km distance band. *Incidence rate = number of cases per 100 people
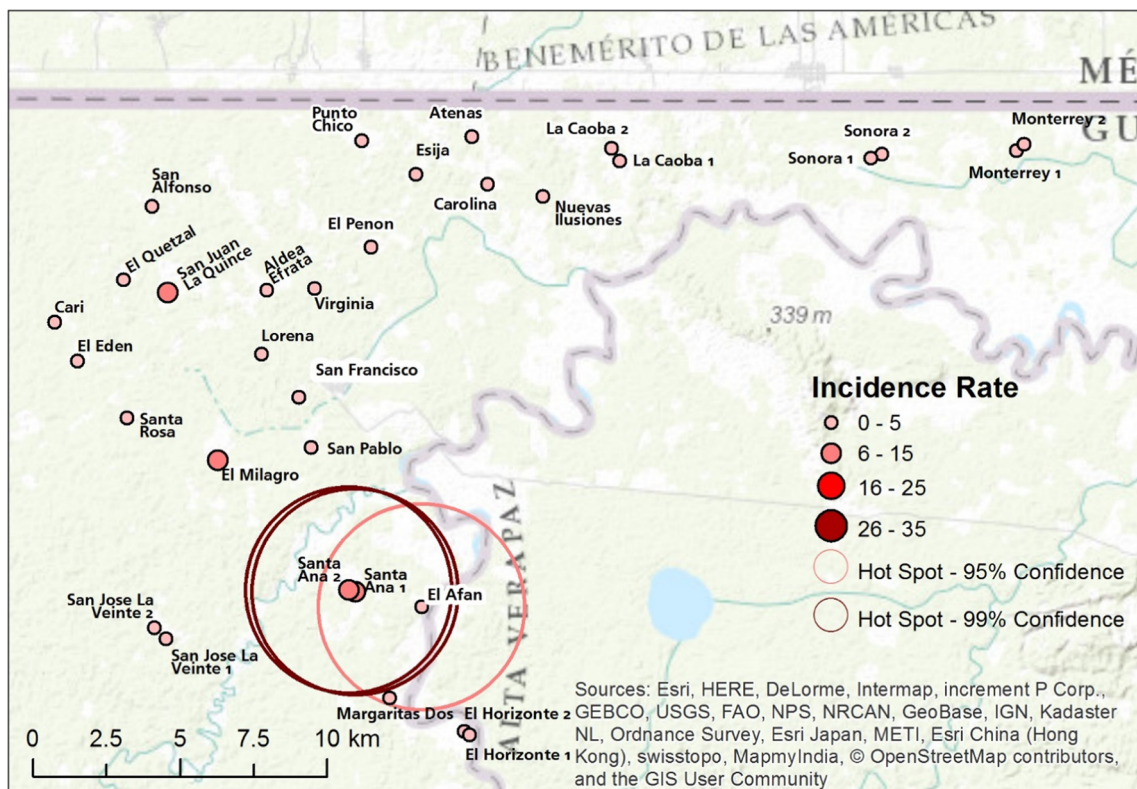
**Fig. 11** Map of villages showing results of the Getis-Ord $G^*(d)$ statistic for post-intervention CT3 (conducted between October and November which correspond to the end of the rainy season and less cases of malaria may occur compared to the middle part of the rainy season) using a 3.5-km distance band. *Incidence rate = number of cases per 100 people

same outlier that was observed using the 3.5-km distance band, while the $G^*(d)$ statistic revealed one cluster of high values of malaria incidence in the central part of the study area that was not detected using the 3.5-km distance lag.

### Distance and significant clustering according to the local Moran's $I$ and $G^*(d)$ statistics

The comparison between the local Moran's $I$ and $G^*(d)$ tests in terms of the number of significant clusters assessed at different distance lags for each of the three CTs indicates that results are similar, although they do not always coincide (Table 5). Results suggest that a higher number of significant clusters of high values (hot spots in $G^*(d)$) are detected with $G^*(d)$ at all distance bands as compared to the local Moran's $I$. Another important difference between the two tests appears from the results of the analysis of clusters of low values of malaria incidence (or cold spots). No significant results were obtained using the local Moran's $I$ test, while significant cold spots were revealed by the $G^*(d)$ in CT1 and CT2 and at higher distance bands (i.e., 5.5 km).

Besides these differences, for both tests, the 3.5-km distance band provided more consistent results than the other distances, and a higher number of significant clusters of high values (or hot spots) were identified in CT1 as compared to

CT2 and CT3. In addition, a common pattern in the spatial distribution of clusters is evident from the results of the two tests not only in terms of the number of significant clusters but

**Table 5** Number of significant clusters of high or low values (for local Moran's $I$) and number of significant hot spots and cold spots (Getis-Ord $G^*(d)$)

| CT1 | | | | |
|---|---|---|---|---|
| Distance | Local Moran's $I$ | | Getis-Ord $G^*(d)$ | |
| | Cluster—high | Cluster—low | Hot spot[a] | Cold spot[a] |
| 3.5 km | 4 | 0 | 5 | 0 |
| 4.5 km | 3 | 0 | 5 | 0 |
| 5.5 km | 2 | 0 | 6 | 2 |
| CT2 | | | | |
| 3.5 km | 1 | 0 | 0 | 0 |
| 4.5 km | 1 | 0 | 1 | 4 |
| 5.5 km | 1 | 0 | 1 | 4 |
| CT3 | | | | |
| 3.5 km | 2 | 0 | 3 | 0 |
| 4.5 km | 1 | 0 | 2 | 0 |
| 5.5 km | 0 | 0 | 1 | 0 |

[a] Only results using 99 and 95% CI are included in the table

also in terms of the geographic location of the clusters in the study area.

## Discussion

This study describes the pattern of malaria distribution in Ixcán, Guatemala, both spatially among villages and temporally over three cross-sectional surveys using malaria incidence data collected during the ITN efficacy study. In terms of spatio-temporal variations in incidence rates, a progressive reduction was observed from CT1 to CT3 in most villages, except for a few locations in the central part of the study area. These findings were also supported by the result of the analysis of the temporal trend for the global spatial association of malaria rates, which showed a significant negative trend of clustering of malaria rates with time globally (over the whole study area). This means that the spatial distribution of malaria rates became progressively less clustered or aggregated as time went by. This negative temporal trend became more pronounced in CT3, as demonstrated by the $p$ value for the global Moran's $I$ which was not significant. This pattern could be partially explained by the introduction of ITNs in CT3, which may have had the effect of reducing clustering of malaria and dispersing cases more equally over the area.

In terms of the results of the spatial analyses, it was observed that rates of malaria differ both spatially and temporally, since clusters of high values of malaria incidence (hot spots) in each of the three CTs were detected in different parts of the study area (the northern and north-western area in CT1, the western area in CT2, and the southern area in CT3) and cold spots were observed in the south and in the north-east in CT1 and CT2 (with higher distance bands), respectively. Overall, it can be easily observed that more clusters were detected in CT1 than in CT2 and CT3. This may be partly explained by the fact that in CT1, more cases of malaria were reported (CT1 was conducted between September and October during the rainy season when more cases of malaria are expected) as compared to CT2 and CT3, which were conducted toward the end of the rainy season and during the dry season, respectively; therefore, fewer cases of malaria are expected to occur. The findings of this spatial analysis are more consistent with a context of unstable, seasonal, and sporadic malaria transmission (Bejon et al. 2010; Hui et al. 2009; Yeshiwondim et al. 2009) than with one of stable malaria transmission in which the location of hot spots or cold spots over a relatively short period of time (approximately 1 year in this study) would be less likely to vary considerably (Bousema et al. 2010). In addition, the results of the spatial analysis only partially coincided with the areas of highest rates of malaria (Fig. 3), indicating that areas of statistically significant clusters are not always readily identifiable from a mere observation of malaria rates distribution. The results also

confirm the unpredictability of malaria distribution in areas of unstable transmission, thus representing a greater challenge for malaria control efforts.

The spatial and temporal variations in malaria incidence observed in this study may have resulted from a combination of factors as follows. It is possible that variations in the distribution of areas of significant clusters of malaria incidence among the CTs were due to differences in climate (Paaijmans et al. 2009, 2010; Patz and Olson 2006) (CTs were conducted in different times of the year during which the temperatures and rainfalls vary, though not markedly) or in other local ecological characteristics, such as the distance to forests, swamps, and agricultural lands, the amount of rainfall, variations in temperature, and altitude (Guthmann et al. 2002; Hakre et al. 2004; Prothero 1995; Yeshiwondim et al. 2009). There is evidence that climatic events linked to El Niño, such as lower rainfall and higher temperatures, have been associated with higher incidence of malaria (Mantilla et al. 2009; Medina et al. 2008); therefore, a marked difference in the spatial distribution of clusters of malaria incidence from year to year (as in the comparison between CT1 and CT3) may be the consequence of regional climate anomalies. The climate-altitude relationship, a major element that can impact malaria transmission, is not believed to play a significant role in the distribution of clusters, since the range of elevations of villages is relatively narrow (approximately between 150 and 250 m above the sea level) and it is likely that only larger gradients in altitude can affect malaria transmission (Bødker et al. 2003; Maxwell et al. 2003; Minakawa et al. 2002). Due to the central role that environmental and geographical characteristics may play on malaria transmission, further research in this region of Central America is warranted.

Another important aspect in the observed variations of cluster distribution is the extent of the impact of malaria control activities in the area (Abeku et al. 2003). One control village (El Milagro) was identified as an outlier of high malaria incidence according to the local Moran's $I$ test for CT3 and one intervention village (Santa Ana), located next to a control village (El Afan) that was identified as a hot spot, was also a hot spot for malaria incidence as per the $G^*(d)$ test in CT3, suggesting that close proximity of an intervention village to a control village (less than 3 km in this case) may increase the risk of malaria in the intervention village. Even though results suggest that malaria control through the use of ITNs (unpublished data) had a marginal impact on the distribution of malaria clusters in this study (only two events that may have been linked to malaria control measures were described), it is essential to consider this factor in the evaluation of the results of a spatial analysis.

The observed variations in terms of the location of identified clusters across the CTs may also be partly explained by the fact that individuals that were infected with malaria in one CT were less susceptible in subsequent CTs and they may

have had undetectable asymptomatic infections (Lennon et al. 2016). As a result, it is possible that significant clusters were detected in areas where the population was more vulnerable to malaria infection. While this hypothesis is not fully supported by surveillance data since the relationship between low transmission intensity of malaria and individuals' immunity has not been well characterized (Doolan et al. 2009; Rolfes et al. 2012), further research in this field is warranted. As far as parasite species is concerned, the higher proportion of *P. falciparum* cases in CT1 as compared to CT3 might be related to a lower temperature in 2000 than in 2001, since it has been proposed that *P. falciparum* tends to prevail over *P. vivax* in the presence of higher temperatures and in the presence of higher transmission intensities as in the case of an epidemic (Gething et al. 2011; Lindsay and Martens 1998).

The findings show the beneficial use of more than one test in spatial analysis, since the available features of each test can provide additional valuable information. Both the local Moran's $I$ and the $G^*(d)$ statistics are widely used in spatial analysis, and results obtained from both tests strengthen the validity of results interpretation. Overall, results from the two tests were similar, although, in contrast to the local Moran's $I$, the $G^*(d)$ resulted in the detection of cold spots at higher distance bands. One important benefit of the use of the local Moran's $I$ is the identification of spatial outliers, which may provide essential information in terms of trends of malaria distribution for malaria control.

The selection of the most meaningful distance band to define an area surrounding a village as its neighbor can be subjective, even though it should be based on the evaluation of the local epidemiological, ecological, and entomological context. In this study, the minimum distance required so that each village had at least one neighboring village was 3.2 km; therefore, we had to select a distance that was at least equal to or higher than 3.2 km. According to the test of global spatial autocorrelation, 3.5 km was the distance band at which the non-random distribution of features was maximized, meaning that the probability of detecting spatial clusters or outliers was highest at that distance. This distance was also consistent with the flying behavior of mosquitoes and with the distribution of ITN and control villages for CT3 (this allows for the assessment of neighboring ITN and control villages in the spatial analysis), although the most central area had a high concentration of ITN villages for which the 3.5-km distance band was not sufficient to reach a control village. This distance band was also chosen in other studies on the spatial analysis of malaria in Latin America (Caldas de Castro et al. 2007; Grillet et al. 2010), adding strength and significance to our decision. To provide a more complete picture, we also presented results of tests for larger distance bands, although distances longer than 5 km may not be suitable for the geographical and entomological characteristics of the study area. To this end, it would have been helpful to have data on the other villages in the area (not all participated in the ITN study) so that we could have also assessed spatial phenomena with shorter distance bands such as 1.5 and 2.5 km.

## Conclusions

Spatial analysis in the field of malaria transmission can reveal hidden patterns otherwise not readily identifiable through an evaluation of malaria incidence distribution. Knowledge of these patterns is particularly beneficial at the village level (as the area of this study) rather than at the departmental or national level, since significant clusters seem to be scattered both spatially over a relatively small area and temporally over a short period of time. With such a high variability, significant clusters in villages should be examined in relation to the local ecological and geographical factors mentioned above, since they may be responsible for such spatial events, and findings can lead to the implementation of more appropriate malaria control programs. Notably, this scenario is probably more applicable to areas of low endemicity where transmission dynamics are dependent upon environmental and entomological factors that display higher variability (e.g., climate and vector behavior) than in areas of stable transmission and higher endemicity. In addition, where malaria transmission is low, understanding the spatial distribution of areas of significantly higher malaria rates may be essential in an attempt to further reduce the number of cases and approach elimination. In such a context, the aid of reliable diagnosis with robust tools and radical treatment is critical in the attempt to reduce the reservoirs of infection and should always be promoted, particularly in areas undergoing malaria pre-elimination and elimination.

## Compliance with ethical standards

**Conflict of interest** The authors declare that they have no conflicts of interest.

**Ethical approval** The study was approved by the Ethics Committee of the Universidad del Valle de Guatemala on July 3, 2000 and the permission to analyze the data was granted by the Ethics Committee of the University of Texas Health Science Center at Houston on August 14, 2015 (permit code HSC-SPH-15-0551). All procedures performed in studies involving human participants were in accordance with the ethical standards of the institutional and/or national research committee and with the 1964 Helsinki declaration and its later amendments or comparable ethical standards.

**Informed consent** Informed consent was obtained from all individual participants included in the study.

# References

Abeku TA, van Oortmarssen GJ, Borsboom G, de Vlas SJ, Habbema J (2003) Spatial and temporal variations of malaria epidemic risk in Ethiopia: factors involved and implications. Acta Trop 87(3):331–340. https://doi.org/10.1016/S0001-706X(03)00123-2

Achee NL, Grieco JP, Andre RG, Rejmankova E, Roberts DR (2007) A mark-release-recapture study to define the flight behaviorsof *Anopheles vestitipennis* and *Anopheles albimanus* in Belize, Central America. J Amer Mosq Control Assoc 23(3):276–282. https://doi.org/10.2987/8756-971X(2007)23[276:AMSTDT]2.0.CO;2

Anselin L (1995) Local indicators of spatial association—LISA. Geogr Anal 27(2):93–115. https://doi.org/10.1111/j.1538-4632.1995.tb00338.x

Bejon P, Williams TN, Liljander A, Noor AM, Wambua J, Ogada E, Olotu A, Osier FHA, Hay S, Färnert A, Marsh K (2010) Stable and unstable malaria hotspots in longitudinal cohort studies in Kenya. PLoS Med 7(7):915. https://doi.org/10.1371/journal.pmed.1000304

Bødker R, Akida J, Shayo D, Kisinza W, Msangeni H, Pedersen E, Lindsay S (2003) Relationship between altitude and intensity of malaria transmission in the Usambara Mountains, Tanzania. J Med Entomol 40(5):706–717. https://doi.org/10.1603/0022-2585-40.5.706

Bousema T, Drakeley C, Gesase S, Hashim R, Magesa S, Mosha F, Otieno S, Carneiro I, Cox J, Msuya E, Kleinschmidt I, Maxwell C, Greenwood B, Riley E, Sauerwein R, Chandramohan D, Gosling R (2010) Identification of hot spots of malaria transmission for targeted malaria control. J Infect Dis 201(11):1764–1774. https://doi.org/10.1086/652456

Caldas de Castro M, Singer BH (2006) Controlling the false discovery rate: a new application to account for multiple and dependent tests in local statistics of spatial association. Geogr Anal 38(2):180–208. https://doi.org/10.1111/j.0016-7363.2006.00682.x

Caldas de Castro M, Sawyer DO, Singer BH (2007) Spatial patterns of malaria in the Amazon: implications for surveillance and targeted interventions. Health Place 13(2):368–380. https://doi.org/10.1016/j.healthplace.2006.03.006

Carter R, Mendis KN, Roberts D (2000) Spatial targeting of interventions against malaria. Bull World Health Organ 78(12):1401–1411

Consejo Municipal de Desarrollo del Municipio de Ixcan, Quiche y Secretaria de Planificacion y Programacion de la Presidencia (2010) Plan de desarrollo Ixcan, Quiche. http://www.google.com/url?sa=t&rct=j&q=&esrc=s&source=web&cd=1&ved=0ahUKEwie2Y-2pd_bAhUEZ1AKHRPyBhUQFggnMAA&url=http%3A%2F%2Fwww.segeplan.gob.gt%2Fnportal%2Findex.php2Fbibliotecadocumental%2Fcategory%2F62-quiche%3Fdownload%3D278%3Apdm-playa-grandeixcan&usg=AOvVaw3lQBXOsuYMvLAh3Qx9iI21. Accessed 22 August 2015

Doolan DL, Dobano C, Baird JK (2009) Acquired immunity to malaria. Clin Microbiol Rev 22(1):13–36, **Table of contents**. https://doi.org/10.1128/CMR.00025-08

Esri (2012) Modeling spatial relationships. http://resources.arcgis.com/en/help/main/10.1/index.html#/Modeling_spatial_relationships/005p00000005000000/GUID-729B3B01-6911-41E9-AA99-8A4CF74EEE27/. Accessed 26 August 2015

Fisher H (1923) Report of the health department of the Panama Canal for 1922. Report of the Health Department of the Panama Canal for 1922. Mount Hope

Gething PW, Van Boeckel TP, Smith DL, Guerra CA, Patil AP, Snow RW, Hay SI (2011) Modelling the global constraints of temperature on transmission of *Plasmodium falciparum* and *P. vivax*. Parasite Vector 4(92):4. https://doi.org/10.1186/1756-3305-4-92

Getis A, Ord JK (1992) The analysis of spatial association by use of distance statistics. Geogr Anal 24(3):189–206. https://doi.org/10.1111/j.1538-4632.1992.tb00261.x

Getis A, Ord J (1996) Spatial analysis and modeling in a GIS environment. A research agenda for geographic information science, pp. 157–196

Grillet ME, Barrera R, Martinez JE, Berti J, Fortin MJ (2010) Disentangling the effect of local and global spatial variation on a mosquito-borne infection in a neotropical heterogeneous environment. Am J Trop Med Hyg 82(2):194–201. https://doi.org/10.4269/ajtmh.2010.09-0040

Guthmann J, Llanos Cuentas A, Palacios A, Hall A (2002) Environmental factors as determinants of malaria risk. A descriptive study on the northern coast of Peru. Tropical Med Int Health 7(6):518–525. https://doi.org/10.1046/j.1365-3156.2002.00883.x

Hakre S, Masuoka P, Vanzie E, Roberts DR (2004) Spatial correlations of mapped malaria rates with environmental factors in Belize, Central America. Int J Health Geogr 3(1):6. https://doi.org/10.1186/1476-072X-3-6

Hui FM, Xu B, Chen ZW, Cheng X, Liang L, Huang HB, Fang LQ, Yang H, Zhou HN, Yang HL, Zhou XN, Cao WC, Gong P (2009) Spatio-temporal distribution of malaria in Yunnan province, China. Am J Trop Med Hyg 81(3):503–509. https://doi.org/10.4269/ajtmh.2009.81.503

Instituto Nacional de Electrificacion (2014) Hidroeléctrica Chixoy se presenta como caso de éxito en hidroindustria. http://www.inde.gob.gt/. Accessed 2 September 2015

Instituto Nacional de Sismologia, Vulcanologia, Meteorologia e Hidrologia (2013) Estaciones meteorologicas en Guatemala. http://www.insivumeh.gob.gt/meteorologia/mapa_estaciones2.htm. Accessed 2 September 2015

Jacquez GM (2008) Spatial cluster analysis. In: The Handbook of Geographic Information Science. Blackwell, Malden, pp 395–416

Kitron U (1998) Landscape ecology and epidemiology of vector-borne diseases: tools for spatial analysis. J Med Entomol 35(4):435–445. https://doi.org/10.1093/jmedent/35.4.435

Lennon ME, Miranda A, Henao J, Vallejo AF, Perez J, Alvarez A, Arévalo-Herrera M, Herrera S (2016) Malaria elimination challenges in Mesoamerica: evidence of submicroscopic malaria reservoirs in Guatemala. Malar J 15(1):441. https://doi.org/10.1186/s12936-016-1500-6

Lindsay SW, Martens WJ (1998) Malaria in the African Highlands: past, present and future. Bull World Health Organ 76(1):33–45

Lu C, Chen D, Kou Y (2003) Algorithms for spatial outlier detection. Data Mining, 2003. ICDM 2003. Third IEEE International Conference on Data Mining, 597–600. doi https://doi.org/10.1109/icdm.2003.1250986

Malvisi L (2015) The impact of insecticide-treated bed nets on malaria incidence in Ixcan, Guatemala and the associated identification of spatial clusters of malaria. Texas Medical Center Dissertations (via ProQuest). AAI10027729. http://digitalcommons.library.tmc.edu/dissertations/AAI10027729

Mantilla G, Oliveros H, Barnston AG (2009) The role of ENSO in understanding changes in Colombia's annual malaria burden by region, 1960–2006. Malar J 8(6):1–11. https://doi.org/10.1186/1475-2875-8-6

Maxwell CA, Chambo W, Mwaimu M, Magogo F, Carneiro IA, Curtis CF (2003) Variation of malaria transmission and morbidity with altitude in Tanzania and with introduction of alphacypermethrin treated nets. Malar J 2:28. https://doi.org/10.1186/1475-2875-2-28

Medina CE, Gomez-Enri J, Alonso JJ, Villares P (2008) Water level fluctuations derived from ENVISAT radar altimeter (RA-2) and in-situ measurements in a subtropical waterbody: Lake Izabal (Guatemala). Remote Sens Environ 112(9):3604–3617. https://doi.org/10.1016/j.rse.2008.05.001

Minakawa N, Sonye G, Mogi M, Githeko A, Yan G (2002) The effects of climatic factors on the distribution and abundance of malaria vectors in Kenya. J Med Entomol 39(6):833–841. https://doi.org/10.1603/0022-2585-39.6.833

Narciso R, Estrada D, Escobar P, Reyes M (2013) Caracterizacion departamental—Quiche 2012. Guatemala City, Guatemala: Instituto Nacional de Estadistica. https://www.ine.gob.gt/sistema/uploads/2013/12/09/AwfjjE8PjNlI3D4DnpYnoGmtL7oux9xH.pdf. Accessed 26 August 2015

Ord JK, Getis A (1995) Local spatial autocorrelation statistics: distributional issues and an application. Geogr Anal 27(4):286–306. https://doi.org/10.1111/j.1538-4632.1995.tb00912.x

Ostfeld RS, Glass GE, Keesing F (2005) Spatial epidemiology: an emerging (or re-emerging) discipline. Trends Ecol Evol 20(6):328–336. https://doi.org/10.1016/j.tree.2005.03.009

Paaijmans KP, Read AF, Thomas MB (2009) Understanding the link between malaria risk and climate. Proc Natl Acad Sci U S A 106(33):13844–13849. https://doi.org/10.1073/pnas.0903423106

Paaijmans KP, Blanford S, Bell AS, Blanford JI, Read AF, Thomas MB (2010) Influence of climate on malaria transmission depends on daily temperature variation. Proc Natl Acad Sci U S A 107(34): 15135–15139. https://doi.org/10.1073/pnas.1006422107

Patz JA, Olson SH (2006) Malaria risk and temperature: influences from global climate change and local land use practices. Proc Natl Acad Sci U S A 103(15):5635–5636. https://doi.org/10.1073/pnas.0601493103

Prothero RM (1995) Malaria in Latin America: environmental and human factors. Bull Latin Am Res 14(3):357–365

Rolfes MA, McCarra M, Magak NG, Ernst KC, Dent AE, Lindblade KA, John CC (2012) Development of clinical immunity to malaria in highland areas of low and unstable transmission. Am J Trop Med Hyg 87(5):806–812. https://doi.org/10.4269/ajtmh.2012.11-0530

Verdonschot PFM, Besse-Lototskaya AA (2014) Flight distance of mosquitoes (Culicidae): a metadata analysis to support the management of barrier zones around rewetted and newly constructed wetlands. Limnologica 45:69–79. https://doi.org/10.1016/j.limno.2013.11.002

World Health Organization (2017) World malaria report 2017. World Health Organization, Geneva

Xia J, Cai S, Zhang H, Lin W, Fan Y, Qiu J, Sun L, Chang B, Zhang Z, Nie S (2015) Spatial, temporal, and spatiotemporal analysis of malaria in Hubei Province, China from 2004–2011. Malaria J 14(1): 145. https://doi.org/10.1186/s12936-015-0650-2

Yeshiwondim A, Gopal S, Hailemariam A, Dengela D, Patel H (2009) Spatial analysis of malaria incidence at the village level in areas with unstable transmission in Ethiopia. Int J Health Geogr 8(1):5. https://doi.org/10.1186/1476-072X-8-5